Increasing Reliability of Price Signals in Long Term Energy Management Problems

Guillaume Erbs* Clara Lage† Claudia Sagastizábal‡ Mikhail Solodov§

Abstract

Determining reliable price indicators in the long-term is fundamental for optimal management problems in the energy sector. In hydro-dominated systems, the random components of rain and snow that arrive to the reservoirs have a significant impact on the interaction of the low-cost technology of hydro-generation with more expensive ones. The sample employed to discretize uncertainty changes certain Lagrange multipliers in the corresponding optimization problem that represent a marginal cost for the power system and, therefore, changes the price signals. The effect of sampling in yielding different price indicators can be observed even when running twice the same code on the same computer. Although such values are statistically correct, the variability on the dual output puts at stake economic analyses based on marginal prices. To address this issue, we propose a dual regularization that yields sample-insensitive indicators for a two-stage stochastic model. It is shown that the approach provides the minimal-norm multiplier of the energy management problem in the limit, when certain parameter is driven to zero. The new method is implemented in a rolling horizon mode for a real-life case, representing the Northern European energy system over a period of one year with hourly discretization. When compared to SDDP, an established method in the area, the approach yields a significant reduction in the variance of the optimal Lagrange multipliers used to compute the prices, with respect to different samples.

1 Introduction

Modern energy markets involve a large number of technologies to generate electricity. Finding the best policy with lower prices is a challenging problem that can be faced in several different energy contexts, [21]. This work considers long term problems solved by Independent System Operators and agents in the business to obtain price signals for hydro-dominated electric systems, similar to those addressed in [3], [13], [4]. Hydro-power has the particular capacity of providing a reserve of energy in the form of water in the reservoirs, and since hydro-generation is cheaper than other sources, in places like Brazil and Northern Europe, a sound hydro-power management in the long term is absolutely essential for the proper functioning of the whole energy system.

Uncertainty in this setting plays a prominent role, as streamflow impact on the reservoir volumes, and their level can deeply affect decisions to be taken. These problems are usually solved by sampling methods such as the well-known *Stochastic Dual Dynamic Programming* (SDDP)

*ENGIE, 1 pl. S. de Champlain, 92930 Paris La Défense, France. Email:guillaume.erbs@engie.com

†ENGIE, CIFRE contract with Université de Paris Sorbonne, France; joint PhD with IMPA – Instituto de Matemática Pura e Aplicada, Brazil. Email: clarammlage91@gmail.com

‡IMECC - UNICAMP, 13083-859, Campinas, SP, Brazil. Email: sagastiz@unicamp.br. Adjunct Researcher. Partly supported by CEPID CEMEAI, FAPERJ, and CNPq Grant 306089/2019-0.

§IMPA – Instituto de Matemática Pura e Aplicada, Estrada Dona Castorina 110, Jardim Botânico, Rio de Janeiro, RJ 22460-320, Brazil. Email: solodov@impa.br. Research of this author is supported in part by CNPq Grant 303913/2019-3, by FAPERJ Grant E-26/200.347/2023, and by PRONEX–Optimization.

method [15]; see also [14]. The data is a sample with a set of scenarios, to which some probability is attached. In the optimization problem, the objective function includes thermal generation cost and load-shedding penalties, and in addition to operational constraints, generation must meet the demand along the time horizon. The growth rate of the overall cost with respect to the demand, or long-term marginal cost is used as a price signal, averaging the output over the different scenarios. In energy optimization terms, the price signal is related with the Lagrange multiplier associated at an optimum with the demand constraint.

Having different scenarios for the streamflow results in different generation schedules to attend the demand, and in different price signals. In the energy sector, price signals obtained with fundamental models of the power system are used to guide the business decisions. Our proposal is to reduce dependency on the sample used, by means of the dual regularization introduced in [11]. Suppose the company has two managers, say in two different locations. Each manager determines price signals using a sample of the same size, but not necessarily the *same scenarios*. The underlying belief is that, if the samples are sufficiently large, the multiplier empirical distributions obtained with both samples will be alike. Hence, the two averaged prices will be similar; in some sense, statistically the same. This is clearly desirable since then, as common sense dictates in this situation, our two managers are likely to make similar business decisions. However, this is not what can be observed, even in very simple examples. Being assimilated to a dual variable in an optimization problem, the price signal presents wild variations and can lead to a very different output. In the simple problem we use as an illustration in Sections 3.1 and 3.3, the correct mean price signal is 0, but one manager obtains a positive price while the other manager obtains the negative of the same value, only because of the difference in the respective samples.

In order to address this issue, in [11] a dual regularization approach was introduced to stabilize Lagrange multipliers in two-stage stochastic programs. This is achieved by adding to the recourse function a penalty given by a factor of certain square norm; see Section 3.2. The new recourse function enjoys sound mathematical properties and, in the limit (as the penalizing factor tends to zero), provides primal and dual solutions to the original problem, yielding the minimal norm price signal in the multiplier set. The proposal makes the distribution of obtained multipliers less dependent on the actual sample used in the computations. In what follows, this effect is refered to as SIP (*sample-insensitive pricing*).

The approach is then employed to solve energy generation problems. In a first set of tests, a stylized electricity system is considered, modeling the long-term problem in a two-stage setting. Distributions of non-regularized and regularized Lagrange multipliers are compared to show the impact of the dual regularization. Using the same structure, but adding complexity to the model, in a second set of tests we consider a real-data ENGIE long-term electricity production management problem with 10^6 variables and 10^6 constraints. For a power system with 200 plants, the model covers 1 year and is discretized into hourly steps. Because of the large scale and the practical necessity of solving the problem in week stages at most, a Rolling Horizon approach is employed, dividing the problem in 51 two-stage problems.

Related works and contributions. The stochastic programming literature on stability is abundant when it comes to primal variables; see [10], [9], [12], [2]. The analysis of multipliers, or dual variables, however, is a different matter. The only other study that we are aware of is [22], which deals with a problem in energy optimization from a different perspective. Specifically, [22] proposes a regularization with respect to *total variation* of price signals that yields satisfactory results when a bundle method handles the inexactness. We consider uncertainty as a perturbation of the right-hand side of some equality constraints of the stochastic programming problem (for the energy application, those perturbations are akin to real-time variations of wind generation). We are interested in a SIP approach that controls the instability with respect to samples, and not with respect to time. Tikhonov regularizations have become popular in data science to avoid over-fitting

of samples, most notably in deep learning, see [5, Chapter 7] and our concluding comments. Somewhat similarly, our regularization scheme aims at maintaining low the variance of the perturbation induced by a sampling process.

The contributions of this work are twofold. On the theoretical side, we extend the convergence theorems in [11] to a more general feasible set, with box constraints, as needed for energy management problems. These results establish the link between the dual regularized problem and the original one, and provide a way to find the minimal norm price signal in the multipliers set. Also, we fully solve an analytical example that illustrates the aforementioned price instability and the SIP proposed in this work. The second line of contributions is in the modeling and computational areas. We show the impact of our approach on a real-life case covering the Northern European region. To handle the corresponding long-term multi-stage problem we solve successive regularized two-stage programs with decreasing second stage, in a rolling horizon mode; see [1]. The mechanism moves week by week over a year, solving 53 two-stage stochastic programs in succession (one per week of the year). Each one week two-stage problem is regularized using our approach. The resulting output provides input for the problem of the next week, therefore yielding an implementable policy. We benchmark our results against SDDP by simulating the system operation over a high number of randomly generated scenarios, covering a large spectrum of foreseeable futures. In the numerical assessment we analyze the price distribution as well as the impact of regularization on the reservoirs levels, the hydro-generation, and the interconnections between zones.

Organization of the Paper. This work is organized as follows. The energy management problem and its notation is introduced in Section 2. As our application is for the Northern European market, we focus on this particular energy system, even if the model can also be used for other regions with important participation of hydro-power plants, including the Brazilian case. Section 3 examines the corresponding price signals, illustrating with an analytical example their instability and explaining the dual regularization proposed as a stabilizing mechanism. In particular, Subsection 3.4 is devoted to asymptotic results that describe the behavior of primal and dual regularized solutions when the regularized problem approaches the original one. Sections 4 and 5 present computational experiments. Section 4 analyzes the consequences of dual regularization for price signals of a two-stage energy generation problem. Finally, in Section 5 we present numerical results obtained with our approach for the Northern European energy system. The benchmark includes a comparison of the performance of SDDP against our method, implemented in a rolling-horizon mode.

2 Formulation of the energy management problem

We are interested in the problem of managing in an optimal manner the generation of an energy system, over a time horizon of 12 months, with weekly discretization. Generation optimization problems in the long term can be found in the literature, with variations in the problem to be solved, such as [6], [20], [4].

2.1 System and Nomenclature

Energy systems like the Northern European considered in our numerical experiments, involve several balancing zones, as illustrated by the diagram in Figure 1. A zone can be a country (say, Finland) or a region in a country (say, Norway 1 to Norway 5). Typically, intra-zone constraints are demand satisfaction and water balance equations, while the overall balance of the system is achieved by interconnections between the zones, as represented by the diagram in Figure 1.

The notation for the different elements defining the optimization problem is given below.

Figure 1: Energy system with balancing zones

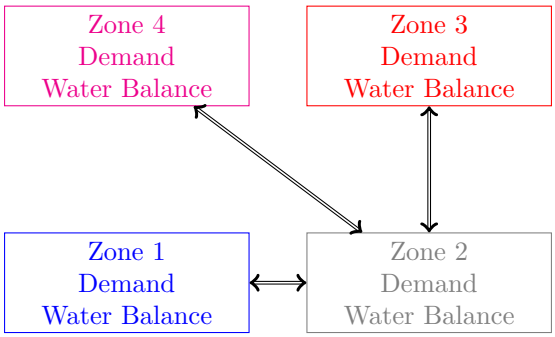

- **Sets:**
  - Scenarios $s \in \mathbb{S}$ each one with probability p^s, representing uncertainty ξ^s on water inflows, changing the hydro power availability.
  - Time steps in the set $\{t \in \mathbb{T}\}$.
  - Balancing zones $\{z_l, l \in \mathbb{L}\}$.
  - A zone z_l has thermal power plants $\{i \in \mathbb{I}_l\}$ and hydro-plants $\{j \in \mathbb{J}_l\}$.
  - For each $l \in \mathbb{L}$, $\mathbb{F}_l$ is a set of zones connected with zone z_l, to import or export energy. When the zone has no connections, this set is empty.
- **Variables at time t:**
  - A hydro-plant $j \in \mathbb{J}_l$ has reservoir level v_j^t (at the end of the stage) and spillage sp_j^t.
  - The generated energy of thermal and hydro-power plants gt_i^t and gh_j^t, respectively.
  - For each $l \in \mathbb{L}$ having nonempty set $\mathbb{F}_l$, and for all $l_1 \in \mathbb{F}_l$, the energy exchanged between zones z_l and z_{l_1} is $f_{l \leftrightarrow l_1}^t$.
  - A possible deficit in generation of zone z_l is represented by an artificial power plant in the set $\mathbb{I}_l$, with very high generating cost and large capacity, defined taking into account renewables curtailment.
- **Parameters:**
  - For the reservoir in hydro-plant $j \in \mathbb{J}_l$, the water inflow $\mathcal{I}_j^{t,s} = \mathcal{I}_j^s(\xi^s)$, noting that for $t = 1$ this is a deterministic value: $\mathcal{I}_j^{1,s} = \mathcal{I}_j^1$, the same for all scenarios s. We consider this value as a given initial reservoir level, denoted v_j^0. For $t > 1$, different scenarios s have different inflows. The reservoir maximum and minimum levels are $\underline{v}_j$ and $\overline{v}_j$, respectively.
  - For thermal power plant $i \in \mathbb{I}_l$ at time t, its maximum generation capacity $\overline{gt}_i^t$ and unit generation cost C_i^t.
  - The hydro-cost of hydro-power plant $j \in \mathbb{J}_l$ is null, its maximum generation capacity is $\overline{gh}_j^t$, and the factor $\eta_j > 0$ converts the reservoir generated energy into turbined water.
  - The forward flow on interconnection between $l \in \mathbb{L}$ and $l_1 \in \mathbb{F}_l \neq \emptyset$ at time t is $f_{l \leftrightarrow l_1}^t$, the backward flow is $f_{l \leftrightarrow l_1}^t$ with respective maximum and minimum values $\overline{f_{l \leftrightarrow l_1}^t}$, $\underline{f_{l \leftrightarrow l_1}^t}$.

– For zone z_l at time t, the deterministic demand $\mathcal{D}_l^t$.

We now explain how to deal with uncertainty, in two stages.

2.2 Two-stage stochastic programming model

For a fixed scenario s, the deterministic formulation for the problem of interest is

$$\left\{\begin{array}{lllll} \min & \displaystyle\sum_{t\in\mathbb{T}}\sum_{l\in\mathbb{L}}\sum_{i\in\mathbb{I}_l} C_i^t\, gt_i^t & & & \\ \text{s.t.} & \underline{v}_j^t \leqslant v_j^t \leqslant \overline{v}_j^t \text{ and } 0 \leqslant sp_j^t, & & j\in\mathbb{J}, & t\in\mathbb{T} \\ & 0 \leqslant gh_j^t \leqslant \overline{gh}_j, \quad 0 \leqslant \underline{gt}_i^t \leqslant \overline{gt}_i^t, & & j\in\mathbb{J}, i\in\mathbb{I}, & t\in\mathbb{T} \\ & -\underline{f_{l\leftrightarrow l_1}^t} \leqslant f_{l\leftrightarrow l_1}^t \leqslant \overline{f_{l\leftrightarrow l_1}^t}, & & l\in\mathbb{L} : l_1\in\mathbb{F}_l\neq\emptyset & t\in\mathbb{T} \\ & v_j^t - v_j^{t-1} + \eta_j\, gh_j^t + sp_j^t & = & \mathcal{I}_j^{t,s}, \quad j\in\mathbb{J}, & t\in\mathbb{T} \\ & \displaystyle\sum_{j\in\mathbb{J}_l} gh_j^t + \sum_{i\in\mathbb{I}_l} gt_i^t + \sum_{l_1\in\mathbb{F}_l\neq\emptyset} f_{l\leftrightarrow l_1}^t & = & \mathcal{D}_l^t, \quad l\in\mathbb{L}, & t\in\mathbb{T}. \end{array}\right. \tag{1}$$

Demand equation involves no variables $f_{l\leftrightarrow l_1}^t$ for zones z_l without interconnections, since in this case $\mathbb{F}_l = \emptyset$. Note also that feasibility is ensured by the spillage and deficit (the artificial power plant generation), which act as slack variables in the equality constraints, thereby ensuring satisfaction of the important property of relative complete recourse for the stochastic optimization problems. Finally, although the hydro-capacity bound does not depend on t, other sources of energy may have a variable capacity (solar, for example, whose maximum generation levels depend on the season of the year).

For legibility, the stochastic version of the linear program (1) is now cast in an abstract format, more suitable for our developments. To this aim, we adopt a two-stage approach to handle uncertainty, splitting the time steps into two sets, $\mathbb{T}_1 := \{t\in\mathbb{T} : t \leqslant t_1\}$ and $\mathbb{T}_2 := \{t\in\mathbb{T} : t > t_1\}$. Until time t_1 all data is known, with scenarios s corresponding to right-hand side uncertainty, relative to times in $\mathbb{T}_2$:

$$\left\{\begin{array}{lll} \min & \langle F_1, x_1\rangle + \displaystyle\sum_{s\in\mathbb{S}} p^s \langle F_2, x_2^s\rangle & \\ \text{s.t.} & 0 \leqslant x_1 \leqslant b_1 & \\ & 0 \leqslant x_2^s \leqslant b_2 & \text{for } s\in\mathbb{S} \\ & T x_1 + W x_2^s = h^s & \text{for } s\in\mathbb{S}. \end{array}\right. \tag{2}$$

The difference between (2) and the problems considered in [11] is in the upper bounds ($x \leqslant b$). The formulation in [11] corresponds to taking $b = +\infty$. Box constraints were not present in that work but they are necessary in our energy problem. The new setting with more constraints changes the multiplier set and for this reason requires a new convergence analysis, see Theorem 3.2 below.

Our energy management problem (2) has a one-year horizon and is solved in a rolling-horizon mode, considering a sequence of two-stage programs (2), each one with $\mathbb{T}_1$ representing the number of hours in the first week under consideration (and $\mathbb{T}_2$ the rest of the year); details are given in Section 5.1.1 below.

The relation between the abstract notation and the one in (1) is the following. Variables with time index $t \leqslant t_1$ define the first-stage decision vector

$$x_1 := \bigcup_{t\in\mathbb{T}_1} \left\{ \left(v_j^t, sp_j^t, gh_j^t)_{j\in\mathbb{J}_l}, (gt_i^t)_{i\in\mathbb{I}_l}, (f_{l\leftrightarrow l_1}^t)_{l_1\in\mathbb{F}_l\neq\emptyset}\right) : l\in\mathbb{L}\right\}, \tag{3}$$

which is of "here-and-now" type. Since we consider that uncertainty reveals at time t_1, all variables with index $t > t_1$ are of the "wait-and-see" type and, hence, denoted by x_2^s for each scenario s:

$$x_2^s := \bigcup_{t\in\mathbb{T}_2} \left\{ \left(v_j^{t,s}, sp_j^{t,s}, gh_j^{t,s}\right)_{j\in\mathbb{J}_l}, \left(gt_i^{t,s}\right)_{i\in\mathbb{I}_l}, \left(f_{l\leftrightarrow l_1}^{t,s}\right)_{l_1\in\mathbb{F}_l\neq\emptyset}\right) : l \in \mathbb{L} \right\}. \tag{4}$$

The objective in (1) is likewise split, so that we have vectors F_1 and F_2 of appropriate dimensions satisfying

$$\sum_{t\in\mathbb{T}_1}\sum_{l\in\mathbb{L}}\sum_{i\in\mathbb{I}_l} C_i^t gt_i^t = \langle F_1, x_1\rangle \quad \text{and} \quad \sum_{t\in\mathbb{T}_2}\sum_{l\in\mathbb{L}}\sum_{i\in\mathbb{I}_l} C_i^t gt_i^{t,s} = \langle F_2, x_2^s\rangle \ . \tag{5}$$

In a similar manner, the box constraints in (1), written for x_1 and x_2^s, are rewritten as

$$x_1 \leqslant b_1 \quad \text{and} \quad x_2^s \leqslant b_2\,, s \in \mathbb{S}\,,$$

taking appropriate vectors b_1 and b_2. Although not present in (1), explicit upper bounds for the spillage and interconnections (variables sp_j^t and $f_{l\leftrightarrow l_1}^t$) can be obtained from the water balance and demand equality constraints.

Finally, notice that in (1) only the water balance equations couple time steps. In particular, for $t = t_1 + 1$, this gives an equality coupling components of x_2^s with components of x_1:

$$v_j^{t_1+1,s} - v_j^{t_1} + gt_j^{t_1+1,s} + sp_j^{t_1+1,s} = \mathcal{I}_j^{t_1+1,s}, j \in \mathbb{J}_l\,, l \in \mathbb{L}\,. \tag{6}$$

In two-stage stochastic programming, the coupling between here-and-now and wait-and-see variables defines an affine relation

$$Tx_1 + Wx_2^s = h^s\,,$$

for abstract right-hand side terms h^s and technology and recourse matrices T and W of appropriate dimensions. The water balance constraints (6) define some lines of this abstract equation. Similarly, the demand equation:

$$\sum_{j\in\mathbb{J}_l} gh_j^t + \sum_{i\in\mathbb{I}_l} gt_i^t + \sum_{l_1\in\mathbb{F}_l\neq\emptyset} f_{l\leftrightarrow l_1}^t = \mathcal{D}_l^t,\ l \in \mathbb{L}\ t \in \mathbb{T}\,, \tag{7}$$

is also incorporated in the constraint $Tx_1 + Wx_2^s = h^s$. As a result, the vector $h^s = h(\xi^s)$ has components given by the right-hand side terms $\mathcal{I}_j^{t,s}$ and $\mathcal{D}_{l_1}^t$.

3 Reliability of price signals

The price signals given by the demand constraint correspond to components of the optimal multiplier associated with the last constraints in (2), with right-hand side vector h^s, for $s \in \mathbb{S}$. As mentioned, a common practice in the energy sector is to average those signals and use the resulting mean price to guide the company business strategies. Sample-sensitive prices are in general undesirable, and the regularization proposed in this work aims at addressing this issue.

We start with a simple example showing that for the energy management problem (2) taking different scenario sets $S_1 \neq S_2$ (with the same cardinality) can yield very different averaged prices. We then extend to the box-constrained setting the stabilizing procedure introduced in [11], and show its convergence.

3.1 An illustrative particular case

Suppose in (2) the right-hand side vector $h_s = \xi_s$ is a particular realization of the continuous variable $\xi \in \mathbb{R}$, with cumulative distribution function denoted by $\mathbb{P}$. The second-stage vectors x_2^s have components $(x_2^+(\xi), x_2^-(\xi)) \in \mathbb{R}^2$, with respective scalar costs F_2^+ and F_2^-, satisfying $F_2^- \geqslant F_2^+ > 0$. We furthermore take $b_1, b_2 = +\infty$, $x_1 \in \mathbb{R}$ and let $T = 1$, $W = [1 \; -1]$ so that the optimization problem is

$$\left\{ \begin{array}{lll} \min & F_1 x_1 + \mathbb{E}[F_2^+ x_2^+(\xi) + F_2^- x_2^-(\xi)] & \\ \text{s.t.} & x_1 \geqslant 0 & \\ & x_2^+(\xi) \geqslant 0 \, , x_2^-(\xi) \geqslant 0 & \text{for a.e. } \xi \\ & x_1 + x_2^+(\xi) - x_2^-(\xi) = \xi & \text{for a.e. } \xi \, , \end{array} \right.$$

with $F_1 > 0$, and where the feasible set is assumed not empty for a.e. ξ. Rewriting this problem in a two-stage formulation,

$$\left\{ \begin{array}{ll} \min & F_1 x_1 + \mathbb{E}[Q(x_1, \xi)] \\ \text{s.t.} & x_1 \geqslant 0 \end{array} \right. , \quad Q(x_1, \xi) := \left\{ \begin{array}{ll} \min & F_2^+ x_2^+ + F_2^- x_2^- \\ \text{s.t.} & x_2^+, x_2^- \geqslant 0 \\ & x_2^+ - x_2^- = \xi - x_1 \end{array} \right. \tag{8}$$

gives, by Linear Programming duality, that

$$Q(x_1, \xi) := \left\{ \begin{array}{ll} \max & \pi(\xi - x_1) \\ \text{s.t.} & -F_2^- \leqslant \pi \leqslant F_2^+ \, . \end{array} \right.$$

Therefore, the optimal multiplier associated with the affine constraint in (8) is

$$\pi(x_1, \xi) := \left\{ \begin{array}{cl} -F_2^- & \text{if } \xi - x_1 < 0 \\ \text{any element in } [-F_2^- , F_2^+] & \text{if } \xi - x_1 = 0 \\ F_2^+ & \text{if } \xi - x_1 > 0 \, . \end{array} \right. \tag{9}$$

The recourse function can be written as

$$Q(x_1, \xi) = F_2^- \max(x_1 - \xi, 0) + F_2^+ \max(\xi - x_1, 0),$$

yielding the explicit form for the expected value:

$$\mathbb{E}[Q(x_1, \xi)] = F_2^- \mathbb{P}(\xi \leqslant x_1) + F_2^+ \mathbb{P}(\xi \geqslant x_1) = F_2^+ + (F_2^- - F_2^+) \mathbb{P}(\xi \leqslant x_1) \, .$$

Then problem (8) boils down to

$$\min_{x_1 \geqslant 0} F_1 x_1 + \mathbb{E}[Q(x_1, \xi) = F_2^+ + \min_{x_1 \geqslant 0} F_1 x_1 + (F_2^- - F_2^+) \mathbb{P}(\xi \leqslant x_1) \, .$$

The cumulative distribution $\mathbb{P}(\xi \leqslant \cdot)$ is a non-decreasing function. Since, in addition, $F_1 > 0$ and $F_2^- \geqslant F_2^+$ by assumption, the minimizer is $\bar{x}_1 = 0$. The corresponding optimal price distribution is

$$\bar{\pi}(\xi) = \left\{ \begin{array}{cl} -F_2^- & \text{if } \xi < 0 \\ \text{any element in } [-F_2^- , F_2^+] & \text{if } \xi = 0 \\ F_2^+ & \text{if } \xi > 0 \, . \end{array} \right. \tag{10}$$

For simplicity, let $F_2^- = F_2^+ = F_2$ and suppose that ξ has a symmetric probability distribution $\mathbb{P}$. Then the continuous price signal for (8) has mean and variance

$$\mathbb{E}[\bar{\pi}(\xi)] = 0 \quad \text{and} \quad \mathbb{V}\mathrm{ar}[\bar{\pi}(\xi)] = \mathbb{E}[\bar{\pi}(\xi)^2] = F_2^2 \, . \tag{11}$$

However, those values can vary wildly, because the model is not sample-insensitive regarding prices. The phenomenon is illustrated by the following example.

If the problem arises in a company with Manager 1 sampling only negative numbers while Manager 2 samples only positive numbers, then $S_1 \subset \mathbb{R}_-$ and $S_2 \subset \mathbb{R}_+$ will respectively result in

$$\begin{array}{llllll} \forall s \in \mathbb{S}_1 & \bar{\pi}_1(\xi^s) = -F_2 & \Longrightarrow & \mathbb{E}[\bar{\pi}_1] = -F_2 & \text{and} & \mathbb{V}ar[\bar{\pi}_1] = 0 \\ \forall s \in \mathbb{S}_2 & \bar{\pi}_2(\xi^s) = \ F_2 & \Longrightarrow & \mathbb{E}[\bar{\pi}_2] = \ F_2 & \text{and} & \mathbb{V}ar[\bar{\pi}_2] = 0\,. \end{array} \tag{12}$$

These are very different (and wrong) empirical signals, no matter how large the samples are.

Of course, this example illustrates an extreme case and any intermediate situation between the most wrong one (as above) and "right" ones (with S_1 and S_2 containing the same number of positive and negative numbers) are possible. In this sense, the sampling method certainly has an impact and can reduce variance. Nevertheless, the stochastic nature of the energy problem (2) still remains, making the issue of computing SIP a real concern for decision makers.

3.2 Dual Regularization of Two-Stage Problems

We now extend to the box-constrained setting the stabilization device proposed in [11], to obtain multipliers with minimum norm. We consider the problem in two levels, presenting first the non-regularized recourse function, and then the regularized one. From the regularized recourse function, it is possible to formulate for one-level the regularized problem.

For the simple example, consider the two-level reformulation of (2),

$$\begin{cases} \min & \langle F_1, x_1 \rangle + \displaystyle\sum_{s \in \mathbb{S}} p^s Q^s(x_1) \\ \text{s.t.} & 0 \leqslant x_1 \leqslant b_1\,, \end{cases} \tag{13}$$

making use of the following recourse function, once more given in primal and dual forms:

$$Q^s(x_1) := \begin{cases} \min & \langle F_2, x_2 \rangle \\ \text{s.t.} & 0 \leqslant x_2 \leqslant b_2 \\ & W x_2 = h^s - T x_1 \end{cases} = \begin{cases} \max & \langle \pi, h^s - T x_1 \rangle - \langle \lambda, b_2 \rangle \\ \text{s.t.} & -\lambda + W^\top \pi \leqslant F_2 \\ & \lambda \geqslant 0\,. \end{cases} \tag{14}$$

This form represents the optimization problem for the two-stage decision x_2. Matrices W and T define the relation between the first and second stage decisions. In the energy context, these matrices represent the water balance equation, and h^s the rain scenario.

Stability of the dual variables with respect to sampling is achieved by considering the following regularized recourse functions, depending on a parameter $\beta > 0$,

$$Q^{\beta,s}(x_1) := \begin{cases} \max & \langle \pi, h^s - T x_1 \rangle - \langle \lambda, b_2 \rangle - \frac{\beta}{2}|\pi|^2 \\ \text{s.t.} & -\lambda + W^\top \pi \leqslant F_2 \\ & \lambda \geqslant 0\,. \end{cases} \tag{15}$$

By construction, the maximizer $\bar{\pi}^{\beta,s}(x_1)$ is unique. Using once again duality,

$$Q^{\beta,s}(x_1) = \begin{cases} \min & \langle F_2, x_2 \rangle + \frac{1}{2\beta}\|h^s - W x_2 - T x_1\|^2 \\ \text{s.t.} & 0 \leqslant x_2 \leqslant b_2\,, \end{cases}$$

whose solutions $\bar{x}_2^{\beta,s}(x_1)$ define an approximation/estimate for the multiplier π:

$$\bar{\pi}^{\beta,s}(x_1) = \frac{h^s - W x_2^{\beta,s}(x_1) - T x_1}{\beta}. \tag{16}$$

Notice that neither the λ-components solving (15) nor the second-stage primal minimizers $\bar{x}_2^{\beta,s}(x_1)$ are guaranteed to be unique. Also, with respect to [11], the upper bounds in our setting introduce the multiplier λ, that was not present in that work.

Going back to the one-level formulation, instead of the linear program (2), we shall solve a quadratic programming problem of the form

$$\begin{cases} \min & \langle F_1, x_1\rangle + \sum_{s\in\mathbb{S}} p^s \Big(\langle F_2, x_2^s\rangle + \dfrac{1}{2\beta} \Big\| h^s - W x_2^s - T x_1 \Big\|^2 \Big) \\ \text{s.t.} & 0 \leqslant x_1 \leqslant b_1 \\ & 0 \leqslant x_2^s \leqslant b_2 \quad \text{for } s \in \mathbb{S}\,. \end{cases} \tag{17}$$

With respect to our energy management problem (1), the rightmost term in the objective function above (with factor $\frac{1}{\beta}$) corresponds to relaxing the water balance and demand equations. These are very important constraints for long term optimal energy management problems.

The choice of β involves a certain trade-off between approximating the non-regularized price distribution and properties of dual-regularized price signals that will be discussed in the following sections. For the numerical experiments in Section 5, with the Nordic energy system, the value of β is chosen so that the total violation is smaller than 1% of the whole hydro-capacity, see Figures 9 and 10 below.

Regarding the tolerance, (here chosen as 1%), it should be specified by the policy-maker. In section 4 ,we discuss choices of β with different tolerance values.

3.3 Back to the analytical case

The effects of our regularization can be examined for the illustrative problem from Section 3. For a symmetric probability distribution and $F_2^- = F_2^+ = F_2$, the stabilized version of (8) is

$$\begin{cases} \min & F_1 x_1 + \mathbb{E}[Q^\beta(x_1,\xi)] \\ \text{s.t.} & x_1 \geqslant 0\,, \end{cases} \quad \text{for } Q^\beta(x_1,\xi) = \begin{cases} \max & (\xi - x_1)\pi - \dfrac{\beta}{2}\pi^2 \\ & -F_2 \leqslant \pi \leqslant F_2\,, \end{cases} \tag{18}$$

which applying formula (16) to case (18) yields a multiplier estimate

$$\pi^\beta(x_1,\xi) := \begin{cases} -F_2 & \text{if } \xi - x_1 < -\beta F_2 \\ \dfrac{\xi - x_1}{\beta} & \text{if } \xi - x_1 \in [-\beta F_2, \beta F_2] \\ F_2 & \text{if } \xi - x_1 > \beta F_2\,, \end{cases} \tag{19}$$

to be compared with the multipliers (9), explicitly computed for the initial problem.

Continuing with two managers, computing multipliers from different samples and now solving the regularized problems, suppose β_k is sufficiently large for the inequality $x_1^k - \beta_k F_2 < 0$ to hold. Even if Manager 1 still samples only negative numbers, now the set S_1 may contain scenarios for which $\xi^s - x_1^k \in [-\beta_k F_2, 0]$, with prices possibly larger than $-F_2$. Similarly, now Manager 2 can sample $\xi^s \in [0, x_1^k + \beta_k F_2]$ for some $s \in \mathbb{S}_2$, thus also considering prices smaller than F_2 when computing the mean. It is therefore likely that the empirical expected prices will be closer to the true mean.

The result below formalizes this setting. Recall from (11) that for the price signal at the solution $\bar{x}_1 = 0$ we have

$$\mathbb{E}[\bar{\pi}(\xi)] = 0 \quad \text{and} \quad \mathbb{V}\mathrm{ar}[\bar{\pi}(\xi)] = F_2^2\,.$$

Proposition 3.1. *Consider the simple problem* (8)*, with minimizer* $\bar{x}_1 = 0$ *and let* $\bar{\pi}(\xi)$ *be an optimal multiplier associated with the affine constraint in the recourse function* $Q(\bar{x}_1, \xi)$*. The*

following holds for $\left(x_1^k, \pi^k(\xi) = \pi^{\beta_k}(x_1^k, \xi)\right)$ *solving the regularized problem* (18)*, written with* $\beta = \beta_k$*:*

$$\lim_{\beta_k \to 0} \mathbb{E}[\pi^k(\xi)] = \mathbb{E}[\bar{\pi}(\xi)] \quad \textit{with} \quad \mathbb{V}\mathrm{ar}[\pi^k(\xi)] \leqslant \mathbb{V}\mathrm{ar}[\bar{\pi}(\xi)]\,. \tag{20}$$

Proof. It is convenient to introduce the short notation

$$\Gamma_-^k := \mathbb{P}(\xi - x_1^k \leqslant -\beta_k F_2)\,, \text{ and } \Gamma_+^k := \mathbb{P}(\xi - x_1^k \geqslant \beta_k F_2)\,,$$

noting that, by the symmetry assumption and the fact that $x_1^k \to \bar{x} = 0$ (see [11, Theorem 3.3]),

$$\lim_{\beta_k \to 0} \Gamma_+^k = \mathbb{P}(\xi \geqslant 0) = \frac{1}{2} = \mathbb{P}(\xi \leqslant 0) = \lim_{\beta_k \to 0} \Gamma_-^k\,. \tag{21}$$

Computing the average of prices (19) yields that

$$\mathbb{E}[\pi^k(\xi)] = F_2(\Gamma_+^k - \Gamma_-^k) + \int_{\frac{\xi - x_1^k}{\beta_k} \geqslant -F_2}^{\frac{\xi - x_1^k}{\beta_k} \leqslant F_2} \frac{\xi - x_1^k}{\beta_k}\, d\mathbb{P}(\xi)\,.$$

To compute the limit, first bound the integral as follows

$$-\Gamma^k F_2 \leqslant \int_{\frac{\xi - x_1^k}{\beta_k} \geqslant -F_2}^{\frac{\xi - x_1^k}{\beta_k} \leqslant F_2} \frac{\xi - x_1^k}{\beta_k}\, d\mathbb{P}(\xi) \leqslant \Gamma^k F_2\,, \text{ for } \Gamma^k := \mathbb{P}(-\beta_k F_2 \leqslant \xi - x_1^k \leqslant \beta_k F_2)\,.$$

Then, using that $\lim_{\beta_k \to 0} \Gamma^k = 0$, passing to the limit as $\beta_k \to 0$ in the inequalities below

$$F_2(\Gamma_+^k - \Gamma_-^k - \Gamma^k) \leqslant \mathbb{E}[\pi^k] \leqslant F_2(\Gamma_+^k - \Gamma_-^k + \Gamma^k)\,, \tag{22}$$

yields, together with (21), that $\lim_{\beta_k \to 0} \mathbb{E}[\pi^k] = 0$, as claimed.

To get the variance expression, since $\mathbb{V}\mathrm{ar}[\pi] = \mathbb{E}[\pi^2] - \mathbb{E}[\pi]^2$, we first compute the first term,

$$\mathbb{E}[\pi^k(\xi)^2] = F_2^2(\Gamma_+^k + \Gamma_-^k) + \int_{\frac{\xi - x_1^k}{\beta_k} \geqslant -F_2}^{\frac{\xi - x_1^k}{\beta_k} \leqslant F_2} \frac{(\xi - x_1^k)^2}{\beta_k^2}\, d\mathbb{P}(\xi)\,,$$

and bound again the integral, as follows:

$$0 \leqslant \int_{\frac{\xi - x_1^k}{\beta_k} \geqslant -F_2}^{\frac{\xi - x_1^k}{\beta_k} \leqslant F_2} \frac{(\xi - x_1^k)^2}{\beta_k^2}\, d\mathbb{P}(\xi) \leqslant \Gamma^k F_2^2\,.$$

Adding the negative of (22) and defining $\Gamma = \max(|\Gamma_+^k - \Gamma_-^k - \Gamma^k|, |\Gamma_+^k - \Gamma_-^k + \Gamma^k|) \leqslant 1$,

$$0 \leqslant \mathbb{E}[\pi^k(\xi)^2] - \mathbb{E}[\pi^k]^2 \leqslant F_2^2 - F_2^2\Gamma^2\,.$$

Since $\mathbb{V}\mathrm{ar}[Z] = \mathbb{E}[Z^2] - \mathbb{E}[Z]^2$ for any random variable Z, this means that

$$\mathbb{V}\mathrm{ar}[\pi^k] \leqslant F_2^2,$$

giving the desired result. □

For this example with explicit solution, the original and regularized price distributions, namely (9) and (19), have the same support (we are not aware if this result holds in general).

The relation in (20) showing that the mean of the regularized prices π^k coincides with the true mean given in (11) is consistent with the general convergence result in [11]. The variational interpretation in [11, Prop.2.1] characterizes the regularized prices as extended Lagrange multipliers using the parametric version of Fermat rule in [17, Ex. 10.12].

The impact of the regularization regarding sample-insensitivity is shown numerically in Figure 3 below. We consider a normal distribution $\xi \sim \mathcal{N}(0, 10)$, $F_2 = F_1 = 5$, and samples $\Xi = \{\xi^1, \dots, \xi^{\mathbb{S}}\}$ with $S = 200$ elements. We fix $\beta = 1$, and compute the numerical value for the multiplier $\bar{\pi}$ and its estimate $\bar{\pi}^\beta$, given in (9) and (19). The respective histograms are shown in Figure 2.

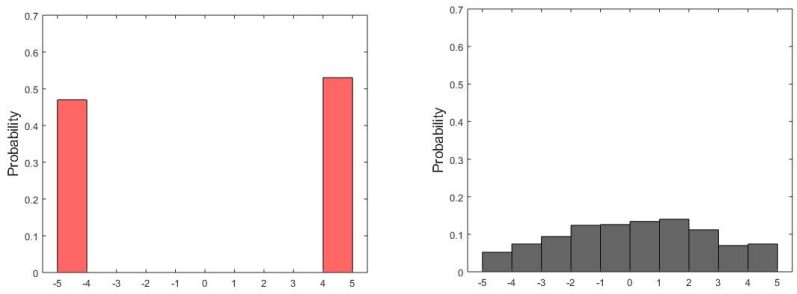

Figure 2: Non-regularized (left) and regularized (right) price signal distributions

The histograms are consistent with the theory: on the left, the values of $\bar{\pi}$ oscillate between -5 and 5, (that is, $-F_2$ and F_2); on the right, the distribution of $\bar{\pi}^\beta$ is smoother.

To see the impact of regularization on the expected value and variance we repeated the same test with different samples Ξ^n, $n \in \{1, \dots, N\}$ for $N = 40$.

The distribution of $\bar{\pi}^\beta$ is computed using $\bar{x}_1^\beta$, the regularized primal solution for the one-level regularized problem (18). The expected value and variance for the $N = 40$ samples are reported in Figure 3.

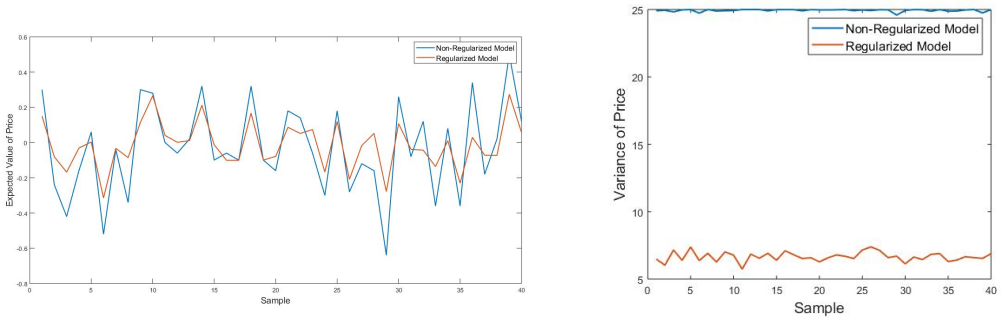

Figure 3: Expected value and variance for 40 samples

Clearly, results cannot match exactly the theoretical ones because we are using a normally distributed finite sample, instead of the continuous normal distribution. Notwithstanding, the left plot in Figure 3 confirms that the expected value is around zero, with the non-regularized model exhibiting a higher variability. On the right plot, on the other hand, we see that when $\beta = 0$ the variance indeed stays close to $25 = 5^2 = F_2^2$, being significantly smaller for the regularized model.

3.4 Asymptotic properties of the dual regularization

The convergence theory in [11] shows that, as $\beta \to 0$, the multiplier estimates converge to a multiplier of the original problem, that has minimal norm. That work considers more general quadratic objective functions, including possibly nonconvex, but, as already mentioned, [11] only deals with equality and nonnegativity (thus, lower bound) constraints. Changing the structure of the feasible set changes the structure of the set of multipliers. We next show how to adapt the theory for problems with upper bounds as in (2). The results from [11] are in some instances specialized, and in other instances extended, for the current setting.

To cast (2) and (17) in the the setting of [11], suppose the scenario set is $\mathbb{S} := \{1, \ldots, S\}$, and denote by n_1 and n_2 the respective dimensions of x_1, x_2^s defined in (3). We define the vectors

$$x := (x_1, x_2^1, \ldots, x_2^S) \in \mathbb{R}^n, \text{ where } n := n_1 + n_2 S,$$
$$g := (F_1, p^1 F_2, \ldots, p^S F_2) \in \mathbb{R}^n,$$
$$a := (h^1, \ldots, h^S) \in \mathbb{R}^{mS}, b := (b_1, b_2, \ldots, b_2) \in \mathbb{R}^n,$$

and the $mS \times n$ matrix

$$A := \begin{bmatrix} T & W & 0 & \ldots & 0 \\ T & 0 & W & \ddots & \vdots \\ T & \vdots & \ddots & \ddots & 0 \\ T & 0 & \ldots & 0 & W \end{bmatrix}, \tag{23}$$

where m is the dimension of h^s. With this notation, problem (2) becomes

$$\begin{cases} \min & \langle g, x \rangle \\ \text{s.t.} & Ax = a \\ & 0 \leqslant x \leqslant b. \end{cases} \tag{24}$$

The multiplier associated with the constraint $Ax = a$ in (24) is denoted π, while the box-constraint multipliers are denoted by μ and λ, respectively for the lower and upper bounds. The convergence results for our regularization are given below.

Theorem 3.2. *[Primal and dual convergence in the setting of problem* (24)*]*
Consider the penalization problem (17)*, which for* (24) *writes down as*

$$\begin{cases} \min & \langle g, x \rangle + \frac{1}{2\beta}\|Ax - a\|^2 \\ \text{s.t.} & 0 \leqslant x \leqslant b. \end{cases} \tag{25}$$

Let the triplet (x^k, μ^k, λ^k) *denote the optimal primal and dual solutions (Lagrange multipliers) to* (25)*, written with* $\beta = \beta_k$*, and let* $\pi^k := (Ax^k - a)/\beta_k$.

If $\beta_{k+1} < \beta_k$ *for all* k*, and* $\beta_k \to 0$*, the following holds:*

(i) The primal sequence $\{x^k\}$ *is bounded and any of its accumulation points minimizes* (24).

(ii) Let $\{x^{k_j}\} \to \bar{x}$ *as* $j \to \infty$ *and let* $N_{\{0 \leqslant x \leqslant b\}}(\bar{x})$ *denote the cone normal to the box-constraints at* $\bar{x}$*. If the condition*

$$\mathrm{Im}(A^\top) \cap N_{\{0 \leqslant x \leqslant b\}}(\bar{x}) = \{0\} \tag{26}$$

holds, then $\{\mu^{k_j}\}$ *and* $\{\lambda^{k_j}\}$ *are bounded. Moreover, for any accumulation point* $(\bar{\mu}, \bar{\lambda})$ *of the subsequence* $\{(\mu^{k_j}, \lambda^{k_j})\}$*, the corresponding subsequence* $\{\pi^{k_j}\}$ *converges to* $\hat{\pi}$*, the solution of:*

$$\min \frac{1}{2}\|\pi\|^2 \, s.t. \quad g + A^\top \pi - \bar{\mu} + \bar{\lambda} = 0. \tag{27}$$

The point $(\bar{x}, \hat{\pi}, \bar{\mu}, \bar{\lambda})$ *is a primal-dual solution of* (24).

Proof. Item (i) is immediate: Every sequence $\{x^k\}$ generated by the method is automatically bounded (and thus has a convergent subsequence), because the set $X = \{0 \leqslant x \leqslant b\}$ is compact. Then, every accumulation point of $\{x^k\}$ is a solution of (24), by [11, Thm. 3.4].

We proceed to item (ii). By KKT conditions for (25), we have that

$$\begin{gathered} g + \frac{1}{\beta_k} A^\top (Ax^k - a) - \mu^k + \lambda^k = 0, \\ x^k \geqslant 0,\ \mu^k \geqslant 0,\ \langle \mu^k, x^k \rangle = 0, \quad x^k \leqslant b,\ \lambda^k \geqslant 0,\ \langle \lambda^k, x^k - b \rangle = 0. \end{gathered} \tag{28}$$

Recalling the definition of π^k and setting $\nu^k := \lambda^k - \mu^k$, we obtain that

$$g + A^\top \pi^k + \nu^k = 0. \tag{29}$$

Let $\{x^{k_j}\} \to \bar{x}$ as $j \to \infty$. We next prove that the sequence $\{(\mu^{k_j}, \lambda^{k_j})\}$ is bounded. To that end, using the second line in (28), first observe the following:

$$\begin{gathered} (\mu^k)_i > 0 \ \Rightarrow\ x_i^k = 0 \ \Rightarrow\ (\lambda^k)_i = 0,\ \nu_i^k = -(\mu^k)_i < 0, \\ (\lambda^k)_i > 0 \ \Rightarrow x_i^k = b \ \Rightarrow (\mu^k)_i = 0,\ \nu_i^k = (\lambda^k)_i > 0. \end{gathered} \tag{30}$$

From those relations, it is obvious that $\{(\mu^{k_j}, \lambda^{k_j})\}$ is bounded if and only if $\{\nu^{k_j}\}$ is bounded.

Next, similarly to the proof of [11, Thm. 3.4], suppose by contradiction that (28) (and thus (29)) hold with $\|\nu^{k_j}\| \to +\infty$. Passing onto a subsequence, if necessary, let $\{\nu^{k_j}/\|\nu^{k_j}\|\} \to \bar{\nu} \neq 0$. Denote $u^{k_j} = -A^\top \pi^{k_j}/\|\nu^{k_j}\| \in \operatorname{Im} A^\top$. Dividing the equality in (29) by $\|\nu^{k_j}\|$ and passing onto the limit as $j \to \infty$, it follows that

$$u^{k_j} = (g + \nu^{k_j})/\|\nu^{k_j}\| \to \bar{\nu} \neq 0.$$

As $u^{k_j} \in \operatorname{Im} A^\top$, $u^{k_j} \to \bar{\nu}$, and $\operatorname{Im} A^\top$ is closed, we conclude that $\bar{\nu} \in \operatorname{Im} A^\top$.

Observe now that from (30) it follows that

$$\bar{\nu}_i < 0 \ \Rightarrow\ \bar{x}_i = 0 \quad \text{and} \quad \bar{\nu}_i > 0 \ \Rightarrow\ \bar{x}_i = b.$$

This shows that $\bar{\nu} \in N_X(\bar{x})$. As $\bar{\nu} \neq 0$ and $\bar{\nu} \in \operatorname{Im} A^\top$, we obtain a contradiction with (26). It follows that $\{\nu^{k_j}\}$ is bounded. And as already observed from (30), this means that $\{\mu^{k_j}\}$ and $\{\lambda^{k_j}\}$ are bounded. The proof that the corresponding subsequence $\{\pi^{k_j}\}$ converges to $\bar{\pi}$, the solution of (27), is analogous to that in Theorem [11, Thm. 3.4].

□

Some comments are in order about the relations between the statements in Theorem 3.2 and those in Theorems 3.3 and 3.4 in [11]. The fact that all accumulation points of $\{x^k\}$ are solutions to (24) is a standard property of exterior penalty methods, see [11, Thm. 3.1] and accompanying comments. However, the *existence* of accumulation points (i.e., boundedness of $\{x^k\}$) is not automatic. In [11, Thm. 3.3], boundedness of the primal sequence was established under certain assumptions. Note that in the current setting we do not need any assumptions, as (25) has box-constraints (and so its feasible set is compact). Condition (26) can be interpreted as a *partial* Mangasarian–Fromovitz condition; see [11, Thm. 2.1] and the associated comments. Its role is to ensure boundedness of the multipliers associated to box-constraints, while allowing the set of multipliers associated to the equality constraints to be unbounded (and in particular, allow for the matrix A to be not of full rank).

4 Numerical experiments for two-stage energy management problems

We have seen in the analyticial example in section 3.1 indications that price signals associated to dual regularization can present some advantages with respect to the standard two-stage stochastic problem. We now investigate numerically the main characteristics of the distribution of the price signal π^β and compare its distribution with that of the original Lagrange multiplier π.

The test represents the management over two years of a stylized power system, with important participation of hydro-power plants. For each given inflow scenario, the following simplification of model (1) is considered:

$$\begin{cases} \min & \langle C_1, gt_1\rangle + \langle C_2, gt_2\rangle & & \\ \text{s.t.} & \underline{v}_j^t \leqslant v_j^t \leqslant \overline{v}_j^t & j \in \mathbb{J} & t \in \{1,2\} \\ & 0 \leqslant gt_j^t \leqslant \overline{gh}_j^t & j \in \mathbb{J} & t \in \{1,2\} \\ & \overline{v}_j^0 \leqslant v_j^2 & j \in \mathbb{J} & \\ & 0 \leqslant gh_i^t \leqslant \overline{gh}_i^t & i \in \mathbb{I} & t \in \{1,2\} \\ & v_j^t - v_j^{t-1} + gh_j^t = \mathcal{I}_j^t, & j \in \mathbb{J} & t \in \{1,2\} \\ & \sum_{j\in\mathbb{J}} gt_j^t = \mathcal{D}^t & & t \in \{1,2\}, \end{cases}$$

where for each reservoir $j \in \mathbb{J}$ an initial reservoir level v_j^0 is fixed. This level also works as a constraint at the end of the timeline, which is consistent with the fact that we should have similar reservoir levels in the end and beggining of the year. The randomness comes from the inflows $\mathcal{I}_j^{2,s}$ in the second stage, while inflows of the first stage are deterministic. The situation described by this problem is the generation planning with a precise estimation of the inflows in the first year (stage 1) and the necessity of being prepared for different realizations in the next year (stage 2). Considering a discrete number of inflow scenarios, the dual-regularized problem writes as follows:

$$\begin{cases} \min & \langle C_1, gt_1\rangle + \mathbb{E}\Big[\langle C_2, gt_2^{t,s}\rangle + (\frac{1}{2\beta}\sum_{\mathbb{J}} \|v_j^{t,s} - v_j^{t-1} + gh_j^{t,s} - \mathcal{I}_j^{2,s}\|^2) \\ & \qquad\qquad +(\sum_{j\in\mathbb{J}} gt_j^{t,s} - \mathcal{D}_l^t)\Big] & & \\ \text{s.t.} & \underline{v}_j^t \leqslant v_j^t \leqslant \overline{v}_j^t & j \in \mathbb{J} & t \in \{1,2\} \\ & 0 \leqslant gt_j^t \leqslant \overline{gh}_j^t & j \in \mathbb{J} & t \in \{1,2\} \\ & \overline{v}_j^0 \leqslant v_j^2 & j \in \mathbb{J} & \\ & 0 \leqslant gh_i^t \leqslant \overline{gh}_i^t & i \in \mathbb{I} & t \in \{1,2\} \\ & v_j^t - v_j^{t-1} + gh_j^t = \mathcal{I}_j^{t,s} & j \in \mathbb{J} & t \in \{1\}. \end{cases}$$

Due to their relatively small size, the non-regularized and regularized problems are solved with LP and QP solvers respectively.

Test data: In this test we consider $\mathbb{J} = \{1,2\}$, and $\mathbb{I} = \{1,2\}$ totaling 4 power plants in the system. The cost of generation for hydro power-plants is considered to be zero.

The value of β : The important choice of the parameter β is made regarding different levels of tolerance concerning the water balance equation. Recall the relation

$$\bar{\pi}^{\beta,s}(x_1) = \frac{h^s - W x_2^{\beta,s}(x_1) - T x_1}{\beta}. \tag{31}$$

When β is sufficiently small, $\bar{\pi}^{\beta,s}$ approximates the non-regularized distribution $\bar{\pi}^s$. The possible values of $\bar{\pi}^s$ are known by the cost vector $C = (C_1, C_2)$. Therefore, choosing β also allows a reliable estimation of the "lost water" because the water balance equation does not define the available set in the regularized case. We compare this reservoir volume with the initial level of the reservoir. We fix levels of β that correspond to values in 0.5% to 2% of v_j^0 for all $j \in \mathbb{J}$. By this heuristics, the choosen values of β for our case are $\{0.5, 1, 2, 3, 4\}$.

Statistical indicators: In Figure 4 we observe the histograms of price signals for different values of β. The histograms are relative to the price signal of one of the hydro-plants in the system.

We observe that, for small values of β, the regularized price signal approximates well the non-regularized distribution. On the other hand, similarly to the example in section 3.1, the distribution tends to spread in the interval between the original price signal values. For relatively larger values of β, as in Figures 4e, 4f, the price signal distribution tends to concentrate in smaller numbers when compared to the non-regularized distribution. These empirical observations can be identified through the expected value and standard deviation in Table 1

The behaviour presented in Figure 4 and Table 1 highlights that the variance of the price signal distribution decreases when the value of β increases. This obversation leads us to investigate the stability of the price signal distribution with respect to different rain distributions as inputs. Each inflow sample $(J^{2,s})_{s=1}^S$ is associated with a price signal distribution $(\pi^{\beta,s})_{s=0}^S$. Clearly, different inflow samples result in different price signal distributions. In Figure 5 we observe that histograms of regularized price signals are more stable.

These distributions can be compared by, for example, the Total Variation. In Tables 2 and 3, we compare the Total Variation of histograms (the mean of the Total Variation of each pair of histograms) and the maximal price signal for different values of β for two different inflows distributions.

By the Total Variation it is possible to conclude that the illustration in Figure 5 is representative. The dual regularization was able to approximate the price-signal distribution with less variation with respect to the inflow distribution. This empirical result is particularly useful when standard deviation of scenarios is large. Typically, in this case, the distribution of price-signals can vary drastically with respect to samples, even when considering a large number of scenarios. Dual regularization can mitigate this phenomena, preserving the main properties of the original distribution. By the maximal value, a useful parameter in applied energy problems, we observe that for small values of parameter β dual regularization is able to well approximate extremes of the price distribution.

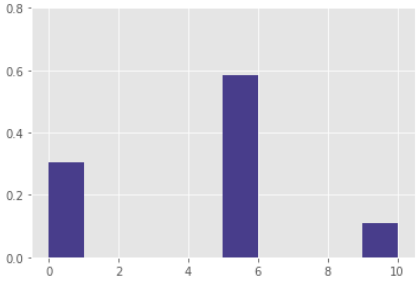

(a) $\beta = 0$

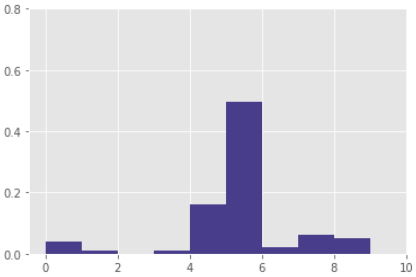

(b) $\beta = 0.5$

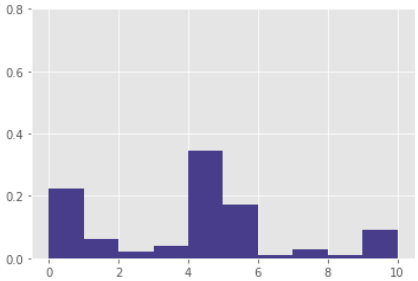

(c) $\beta = 1$

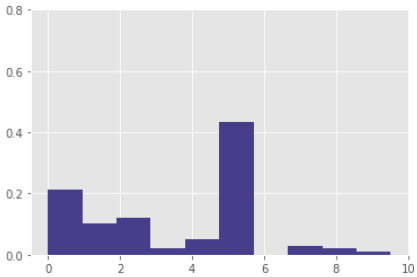

(d) $\beta = 2$

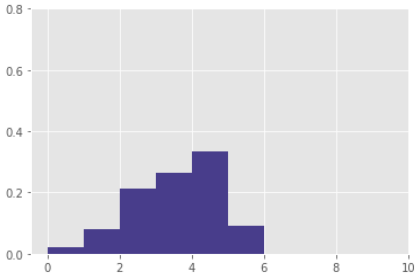

(e) $\beta = 3$

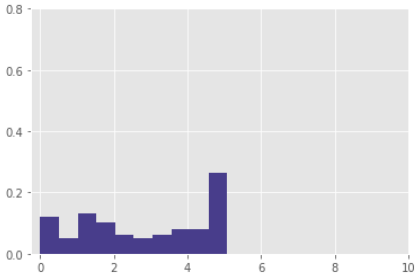

(f) $\beta = 5$

Figure 4: Histograms of price-signals with 100 inflow scenarios for different values of β

Values of β	Expected Value	Standard Deviation
$\beta = 0$	6.1	3.51
$\beta = 0.5$	5.67	2.90
$\beta = 1$	4.48	2.38
$\beta = 2$	3.45	2.09
$\beta = 3$	3.29	1.78
$\beta = 4$	2.65	1.49

Table 1: Main statistical indicators of price signal distribution

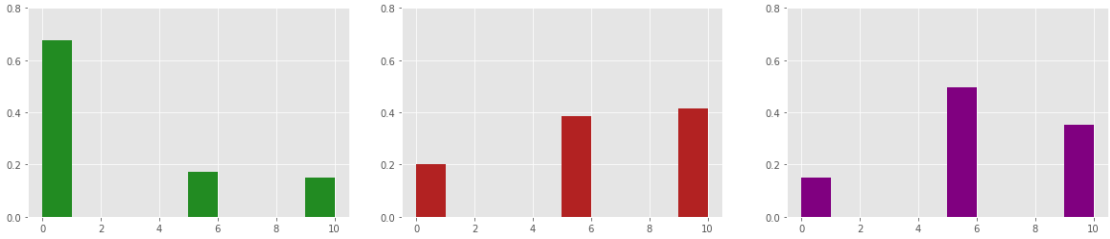

(a) Sample 1 (b) Sample 2 (c) Sample 3

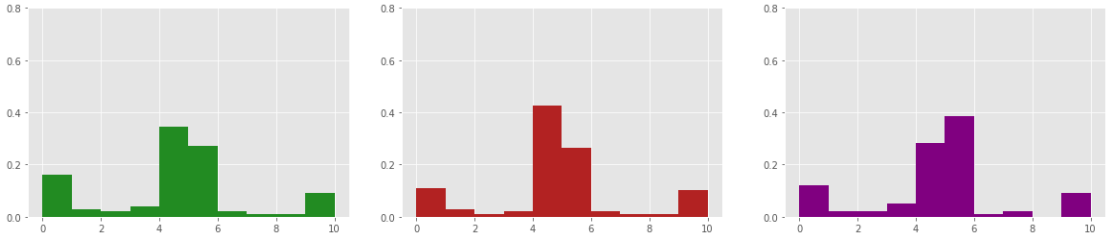

(d) Sample 1 (e) Sample 2 (f) Sample 3

Figure 5: Histograms of price-signals for different samples and $\beta = 1$

Values of β	Total Variation (Mean Pairwise)	Standard Deviation (Mean)	Maximal Price Signal (Mean)
$\beta = 0$	0.31	3.52	10.0
$\beta = 0.5$	0.27	2.96	10.1
$\beta = 1$	0.26	2.53	8.67
$\beta = 2$	0.28	2.11	5.8
$\beta = 3$	0.20	1.88	5.0
$\beta = 4$	0.18	1.12	5.1

Table 2: Mean of the Total Variation of 10 samples of 100 random inflow scenarios with distribution $\mathcal{N}(100, 20)$

Values of β	Total Variation (Mean Pairwise)	Standard Deviation (Mean)	Maximal Price Signal (Mean)
$\beta = 0$	0.49	2.98	9.4
$\beta = 0.5$	0.45	2.91	9.80
$\beta = 1$	0.29	2.79	9.79
$\beta = 2$	0.27	1.93	7.20
$\beta = 3$	0.18	1.51	5.1
$\beta = 4$	0.20	1.12	5.0

Table 3: Mean of the Total Variation of 10 samples of 100 random inflow scenarios with distribution $\mathtt{Lognormal}(3.5, 0.9)$

Constraints violation: One of the main concerns of the regularized model (17) is the violation of constraints, here water balance and demand. We analyse the numerical behaviour of the errors defined below, for different scenarios,

$$\epsilon_{\mathcal{J}}^{\beta,s} = \frac{\mathcal{J}_j^{2,s} - \sum_{\mathbb{J}} v_j^{2,s} - v_j^1 + g h_j^{2,s}}{\mathcal{D}^2}, \quad \epsilon_{\mathcal{D}}^{\beta,s} = \frac{\sum_{\mathbb{J}} g t_j^{2,s} - \mathcal{D}^2}{\mathcal{D}^2}.$$

The normalization with respect to the total demand measures the impact of the violation for the system under consideration. Notice that negative values of the error indicate unattended demand. The graphs in Figure 6 show the constraint violation for the demand, for different values of the parameter β.

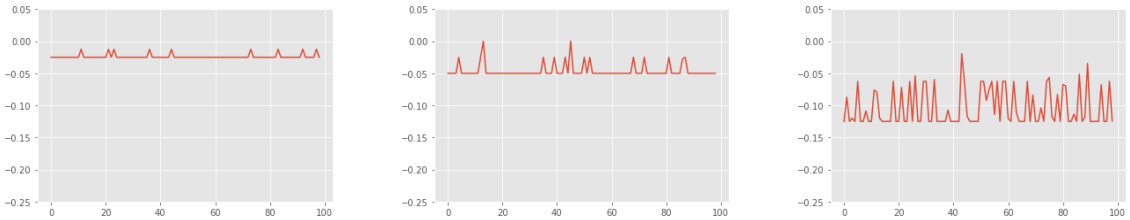

(a) $\beta = 0.1$ (b) $\beta = 1$ (c) $\beta = 4$

Figure 6: Violation of the demand equation with respect to the total demand for 100 inflow scenarios and different values of β.

We observe that, on average, the errors $\epsilon_{\mathcal{D}}^{\beta}$ increase together with β, which is the expected behaviour since the penalization is lower in this case. In percentual terms, for the lower values of β, demand violation is not significant (it is -1.56% for $\beta = 0.1$ and -9.1% for $\beta = 4$ in average).

The graphs in Figure 7, reporting the violation of the water balance equation, show a similar behaviour. A negative value for the error now indicates that the considered inflow was sufficiently large to satisfy the contraint. The constraint violation varies from a mean of 1.87% for $\beta = 0.1$ and 14% for $\beta = 4$.

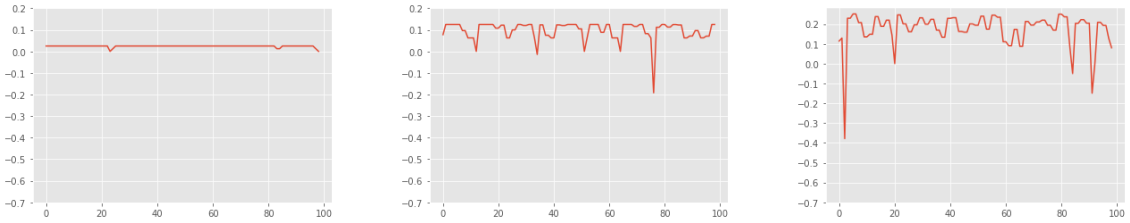

(a) $\beta = 0.1$ (b) $\beta = 1$ (c) $\beta = 4$

Figure 7: Violation of the water balance equation with respect to the total demand for 100 inflow scenarios and different values of β

5 Benchmark for Northern European system

The energy system described in Section 2 has 12 bidding zones. These bidding zones are important since the flow between them is limited. Norway, with 5 zones, has the largest percentage of hydro-energy generation, which amounts to an equivalent of 95% of its demand. Other countries have several different sources of energy. Sweden has a large proportion of nuclear generation, while in

Denmark wind generation amounted to half of its demand in 2014. As in the diagram in Figure 1, imports and exports are handled as interconnections between zones. In total the system has $\mathbb{L} = 30$ balancing zones, $\mathbb{J} = 21$ hydro-power plants, and $\mathbb{I} = 224$ thermal power plants.

In this work, hydro-power plants are assumed to have no generation cost. Our model uses real and estimated values from ENGIE's database for historical inflows, thermal generation and import costs, capacity of each power plant in the system, minimum and maximum level of reservoirs and maximum flow between zones. In this work, the inflow uncertainty was generated by calibrating a log-normal distribution over historical inflow scenarios.

Each stage of the problem corresponds to a week in the year and is subdivided in hours. The hourly subdivision in ENGIE model reflects the system variation during a typical day as a result of intermittent sources such as wind or solar. In this (long-term) model, the hourly variation is revealed for the next seven days, all at once, at the beginning of each week. As such, the corresponding time subdivision is just part of one weekly scenario, it does not represent a separate stage in the multistage stochastic problem.

As usual with multi-stage stochastic programs, the numerical assessment is split into two steps. One defining implementable policies by solving the multi-stage energy problem, and a second phase, simulating the system operation under the policy provided as an output of the optimization step.

5.1 Optimization Phase

Our goal is to compare the price signals obtained by SDDP on the original multi-stage problem with our two-stage regularized approach running in a rolling-horizon mode, denoted below by RRH. A third solver, RH, is the two-stage rolling-horizon algorithm without regularization. The mechanism of rolling horizon put in place for both RH and RRH is described below.

5.1.1 Rolling-horizon Methodology

The time horizon of one year was discretized into $\mathtt{t} = 1, \ldots, 365$ days. At the first hour of each week, the inflow uncertainty of the whole week becomes known. Since the year has 52 weeks, this defines a multi-stage structure of uncertainty, that we cast in our two-stage setting as follows.

We put in place a *rolling-horizon* mode, in which we solve $w = 1, \ldots, 53$ two-stage problems derived from (1) in Section 2. In the w-th two-stage problem, the decision variables of the w-th week are considered in the first stage. The uncertainty of the remaining $w+1, \ldots, 52$ weeks is revealed at once, at the end of the week w and, hence, the corresponding decision variables are considered in the second stage. Since one week has 7 days, the time horizon of the w-th problem covers $\mathbb{T}^w := 7(52 - w + 1)$ days. The output of the w-th two-stage problem provides input for the problem $w + 1$.

With this mechanism, the first-stage components of the decision vector of problem w are in fact decision variables for the w-th week. Accordingly, if $\bar{\mathrm{x}}_1^{\beta;w}$ denotes the first-stage component of a solution obtained for the w-th two-stage problem, then the primal policy

$$\left\{\bar{\mathrm{x}}_1^{\beta;w} : w = 1, \ldots, 52\right\} \tag{32}$$

is *implementable*, as defined in [18]. Another output, close to SDDP pricing mechanism, is the following dual policy, also implementable, that gives a value to water:

$$\left\{ \text{ the cuts for } \mathbb{E}\left[\mathrm{Q}^{\beta,s;w}(\bar{\mathrm{x}}_1^{\beta;w})\right]; w = 1, \ldots, 53\right\} . \tag{33}$$

That is, the cuts of the successive expected recourse functions at a solution, that are also expressed in terms of Lagrangian multipliers (see in the following section (34) and (35)).

Mathematical Formulation We now define mathematically the problem solved in a rolling horizon. In the next sections we shall use this formulation as a reference to explain our simulations.

Following the notation introduced in Section 2 to formulate the energy management problem, for the w-th week we let

$$\mathbb{T}_w = \{t \ : \ 7(w-1) < t \leqslant 7w\}, \text{ and } A_w = \{t \ : \ 7w < t\}.$$

We write the problem for the w-th week as follows:

$$\begin{cases} \min & \displaystyle\sum_{t\in\mathbb{T}_w}\sum_{l\in\mathbb{L}}\sum_{i\in\mathbb{I}_l} C_i^t\, gt_i^t + \mathbb{E}[\mathbb{Q}_w^\beta(v_j^{7w}, \mathcal{I}_j^s)] & \\ \text{s.t.} & \underline{v}_j^t \leqslant v_j^t \leqslant \overline{v}_j^t \text{ and } 0 \leqslant sp_j^t, & j\in\mathbb{J}\,, t\in\mathbb{T}_w \\ & 0 \leqslant gh_j^t \leqslant \overline{gh}_j^t, \quad 0 \leqslant gt_i^t \leqslant \overline{gt}_i^t, & j\in\mathbb{J}\,, i\in\mathbb{I}\,, t\in\mathbb{T}_w \\ & -\underline{f_{l\leftrightarrow l_1}^t} \leqslant f_{l\leftrightarrow l_1}^t \leqslant \overline{f_{l\leftrightarrow l_1}^t}, & l\in\mathbb{L} : l_1\in\mathbb{F}_l \neq \emptyset\,, t\in\mathbb{T}_w \\ & v_j^t - v_j^{t-1} + \eta_j\, gh_j^t + sp_j^t = \mathcal{I}_j^t, & j\in\mathbb{J}\,, t\in\mathbb{T}_w \\ & \displaystyle\sum_{j\in\mathbb{J}_l} gh_j^t + \sum_{i\in\mathbb{I}_l} gt_i^t + \sum_{l_1\in\mathbb{F}_l\neq\emptyset} f_{l\leftrightarrow l_1}^t = \mathcal{D}_l^t, & l\in\mathbb{L}\,, t\in\mathbb{T}_w\,, \end{cases}$$

where $v_j^{7(w-1)}$ is the reservoir level decision that had been made in the $(w-1)$-th week. The inflows $\mathcal{I}_j^t$ for $t\in\mathbb{T}_w$ correspond to a path in the tree of scenarios that is obtained by a uniform random choice in scenario tree.

The regularized recourse functions defined in the second stage are

$\mathbb{Q}_w^\beta(v_j^{7w}, \mathcal{I}_j^s) :=$

$$\begin{cases} \min & \displaystyle\sum_{t\in A_w}\sum_{l\in\mathbb{L}}\sum_{i\in\mathbb{I}_l} C_i^t\, gt_i^t \quad + \tfrac{1}{2\beta}\|v_j^{7w+1} - v_j^{7w} + \eta_j\, gh_j^{7w+1} + sp_j^{7w+1} - \mathcal{I}_j^{7w+1,s}\|^2 & & \\ \text{s.t.} & \underline{v}_j^t \leqslant v_j^t \leqslant \overline{v}_j^t \text{ and } 0 \leqslant sp_j^t, & j\in\mathbb{J}\,, & t\in A_w \\ & 0 \leqslant gh_j^t \leqslant \overline{gh}_j^t, \quad 0 \leqslant gt_i^t \leqslant \overline{gt}_i^t, & j\in\mathbb{J}\,, i\in\mathbb{I} & t\in A_w \\ & -\underline{f_{l\leftrightarrow l_1}^t} \leqslant f_{l\leftrightarrow l_1}^t \leqslant \overline{f_{l\leftrightarrow l_1}^t}, & l\in\mathbb{L} : l_1\in\mathbb{F}_l \neq \emptyset, & t\in A_w \\ & v_j^t - v_j^{t-1} + \eta_j\, gh_j^t + sp_j^t = \mathcal{I}_j^{t,s}\ , & j\in\mathbb{J}\,, & t\in A_w \\ & \displaystyle\sum_{j\in\mathbb{J}_l} gh_j^t + \sum_{i\in\mathbb{I}_l} gt_i^t + \sum_{l_1\in\mathbb{F}_l\neq\emptyset} f_{l\leftrightarrow l_1}^t = \mathcal{D}_l^t, & l\in\mathbb{L}\,, & t\in A_w\,, \end{cases}$$

where $\mathcal{I}_j^{t,s}$ is random and depends on the scenario s. When $\beta = 0$, the constraint moves from the objective function to the feasible set. Note that the sets A_w contain all t such that $t > 7w$, which agrees with the indices in the objective value function $7w+1$ (the first day of the w-th week).

In this notation the sequence $\left\{\bar{x}_1^{\beta;w} : w = 1, \ldots, 52\right\}$ from (32) corresponds to the reservoir level $\bar{x}^{\beta;w} = (v_j^{7w})$, while the cuts for the function $\mathbb{E}\left[Q^{\beta,s;w}(\bar{x}_1^{\beta;w})\right]$ in (33) are expressed in terms of the couple $(\bar{\pi}_{j,k}^{7w+1}, \delta_{it}^w)$, for each iteration k, where $\bar{\pi}_k^{7n+1,k} > 0$, and

$$\bar{\pi}_{j,it}^{7w+1,k} = \frac{1}{S}\sum_s \pi_{j,it}^{7w+1,k,s}, \tag{34}$$

$$\delta_k^w = \frac{1}{S}\sum_s \mathbb{Q}_{w,k}(v_j^{7w}, \mathcal{I}^s) - \sum_j \bar{\pi}_{j,k}^{7w+1,k} v_j^{7w}\,, \tag{35}$$

where (34) is the angular coefficient and (35) the linear coefficient of the cut.

We note that the regularized problem above differs slightly from the abstract formulation (2). The latter includes in the penalization, via the definitions of T and W, both the water balance

and demand constraints. In the problem above, by contrast, we only penalize the water balance, to simplify the implementation. That is, we penalize the equation

$$v_j^{7n+1} - v_j^{7w} + \eta_j gh_j^{7w+1} + sp_j^{7w+1} - \mathcal{J}_j^{7w+1,s}$$

for the w-th week. Recalling the notation of Section 3.2, vector Tx_1 is now represented by $-v_j^{7w}$, which is a vector of the reservoir levels for hydro power plants. And vector Wx_2^s is now: $v_j^{7n+1} + \eta_j gh_j^{7w+1} + sp_j^{7w+1}$, that is, the sum of a vector representing the reservoir levels of hydro power plants v, the generation gh and the spillage sp. The inflow scenario is also a vector: $\mathcal{J}_j^{7w+1,s}$.

For these problems, if the reservoir levels are kept below their maximal capacity, the Lagrange multipliers of the demand and water balance equation coincide (in the figures below, with the reservoir dynamics after the optimization and simulation phases, the maximum capacity is never reached).

Problem dimension The Rolling Horizon approach (RH) for the non-regularized case is composed by S scenarios of inflows $\mathcal{J}^s$. For each one of the 52 weeks, it is necessary to solve a two-stage problem. In the first stage, the decision variable x_1^w (see (3) in detail) has dimension

$$\#\mathbb{T}_w \times \Big(\underbrace{2 \times \sum_{l \in \mathbb{L}} \#\mathbb{J}_l}_{\text{Reservoir/Spill}} + \underbrace{\sum_{l \in \mathbb{L}} \#\mathbb{I}_l + \#\mathbb{J}_l}_{\text{Generation}} + \underbrace{\sum_{l \in \mathbb{L}} \#\mathbb{F}_l}_{\text{Transferences}} \Big), \tag{36}$$

(we use # to indicate the cardinality of the sets). The second stage variable $x_2^{w,s}$, depends on the scenarios $s \in \{1, ..., S\}$ (see equation (4)) and has dimension as (36) replacing $\#\mathbb{T}_w$ by $\#A_w$.

The objective functions F_1 and F_2^2 (see equation (5)) are linear with the same dimensions of x_2 and x_2^s respectively. All variables have box constraints. Each zone have a demand constraint, totaling $\#\mathbb{L}$ demand constraints. Water balance constraints are written per hydro power plant and time, summing, in the first stage $\#\mathbb{T}_w \times \sum_{l \in \mathbb{L}} \#\mathbb{J}_l$ water balance constraints.

The difference between problems for stages 1 and 2, in addition to the set of time $\mathbb{T}_w$ and A_w, is that in the second stage the set of water balance constraints is in the objective function as a sum of square norms. Since there is one water balance constraint for each hydro power-plant, for each one of the zones, the set of these constraints can be seen as a vector of dimension $\sum_{l \in \mathbb{L}} \#\mathbb{J}_l$. Particularly, for $t = 7w + 1$ the equation connects the decision variables x_1^w and x_2^w (for stages 1 and 2). In the first stage, for $t = 7(w-1)$ we have a initial fixed condition that connects the first stage decision x_1^w with the decision from the previous two-stage problem of the Rolling Horizon method, except for time $t = 0$ where we find an initial condition.

Each one of the two-stage problems can solved using the well-known L-Shaped algorithm [19].

5.1.2 Results for the optimization phase

The optimization part of the experiment uses an in-sample set with 30 inflow scenarios and takes $\beta := 7000$ for RRH (below we explain that with this value, the magnitude of the violation incurred by RRH is less then 1% for the whole system). The SDDP method takes one scenario randomly in the forward pass and all the 30 scenarios in the backward pass. The rolling-horizon variants take the same forward scenario, for the different weeks $w = 1, 2, \ldots$, including the 30 scenarios from week $w + 1$ to week 48 in the second stage of the w-th two-stage problem.

The aggregate reservoir management (adding all the hydro-plants), is shown in Figure 8, where colors correspond to the different weeks. The values are normalized with respect to the maximum system capacity.

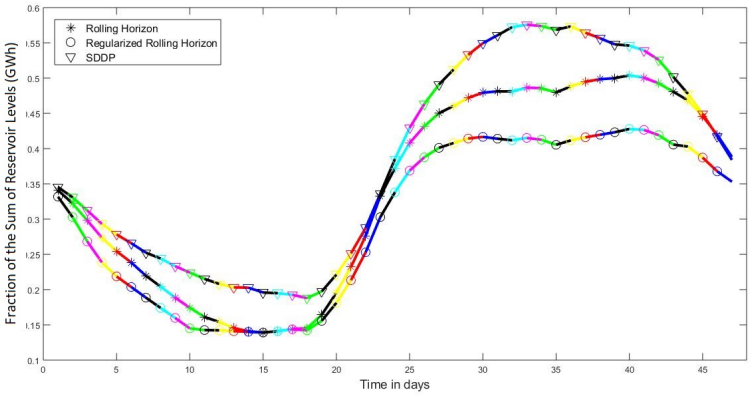

Figure 8: Aggregate reservoir management - optimization phase

Policies for the Rolling Horizon are defined by the first stage solution in equation (32), these policies consider one of the past scenarios as initial level of reservoir and many scenarios as possible rain levels. It is important to explain that the SDDP curve was made running the SDDP algorithm and storing cuts, that estimate the future cost function, until SDDP converges. With the cuts as inputs, we ran a forward path of SDDP following the same path considered by RH and RRH, making a fair comparison between these tree models.

The levels of reservoirs with the rolling-horizon modes are lower, with the RRH using the most of water. Since SDDP sees a larger portion of the scenario tree in the backward pass (not only the tail of the weeks $w+1,\ldots,52$), SDDP water management is more conservative. Regarding the comparison between RRH and RH, that is, one expects to see more relaxed operations for the RRH model. Note that the inequality $Q^{\beta,s}(\cdot) \leqslant Q^{s}(\cdot)$ always holds (the feasible set defining the former is included in the one defining the latter). Having an under-estimation of the future-cost function, RRH tends to be less conservative than RH, keeping less water in the reservoirs.

Since RRH does not consider the water-balance equations, in Figure 9 we examine the gap

$$v_j^t - v_j^{t-1} + \eta_j\, gh_j^t + sp_j^t - \mathcal{I}_j^{t,s}$$

over the first 48 weeks for $s = 1,\ldots,12$ scenarios (different colors in the figure), for two hydro-plants in Norway.

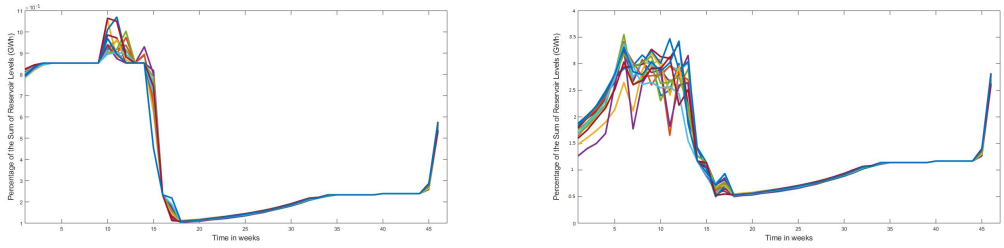

Figure 9: Absolute violation of water balance - Zones 1 and 3 in Norway (left and right)

We note that the system exploits the most the possibility of not satisfying the water-balance equation in the beginning of the year, when inflows are smaller. In order to determine the real extent of the violation, relative to the total hydro-capacity, we use the expression for the multiplier

approximation

$$\pi^{\beta}(\xi) = \frac{Tx_1 + Wx_2(\xi) - h(\xi)}{\beta},$$

to estimate the gap by $\beta\pi^{\beta}(\xi)$. Since $\beta = 7000$ and the price signals are about 10^2, the magnitude of the violation incurred by RRH is of order 10^5. This is consistent with the graphs in Figure 9. The whole hydro-capacity being about 10^7, the gap is less then 1% for the whole system. The mean violation, in relative values, over the 30 scenarios and all the hydro-power plants, is shown in Figure 10 for the first 48 weeks.

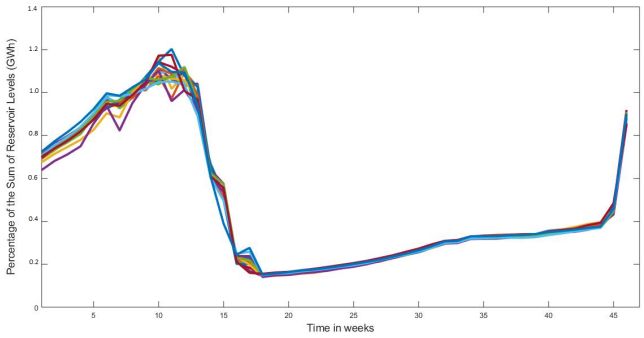

Figure 10: Relative mean violation of water balance in the whole system

5.2 Simulation phase

We now assess the quality of the policies obtained by the three solvers on an out-of-sample set with 200 scenarios. After the optimization phase, we simulate different scenarios as input data and examine the Wasserstein distance between the histograms of the respective price signals. We expect to obtain similar expected values for the three solvers, but a smoother distribution for RRH. A similar measure for the quality of optimal decisions is considered in [8], to assess a proposal to build a scenario tree that preserves certain essential statistical properties. The different trees generated with their approach maintain the optimal value of the considered optimization problem. The rationale is that if the relevant statistical information is captured by the method, the result should not vary too much with the data input. Along these lines, in [7] it is shown that primal regularization does not affect the statistical properties of the solution and the number of iterations required by algorithms based on cutting planes. In our tests, solving the regularized model required slightly more iterations.

The first simulation, here called primal simulation and detailed in section 5.2.1, consists in using the first stage decisions from each one of the 52 weeks w, that is the set:

$$\left\{\bar{x}_1^{\beta;w} : w = 1, \ldots, 52\right\}$$

and to simulate second stage decisions, and Lagrange multipliers, from new inflow scenarios $\mathcal{J}^s$, for $s \in \{1, ..., 200\}$.

The second simulation, here called dual simulation and presented in section 5.2.2, has as objective to compare the distribution of price signals for RH, RRH and SDDP. For RH and RRH, we consider the price signals:

$$\{\bar{\pi}^{\beta;w;s} : w = 1, \ldots, 52, s = 1, , \ldots, 30\},$$

where $\beta = 0$ for RH. $\bar{\pi}^{\beta;w;s}$ for different values of s is, therefore, the distribution of prices signals with respect to 30 scenarios for each one of the weeks in the year. For SDDP we use the dual policies computed in each one of the stages (used in SDDP method to compute cuts for the future-cost function). Similarly, We have a set:

$$\{\tilde{\pi}^{\beta;w;s} : w = 1, \dots, 52, s = 1, , \dots, 30\}$$

of price signals for SDDP.

5.2.1 Primal Simulation

This is the primal policy (32), available only with the rolling-horizon solvers RH and RRH, but not with SDDP. As the latter solver lacks a primal policy, the comparison with SDDP is done in the next section, when assessing the regularized dual policies. To benchmark the histograms of price signals obtained when implementing RH and RRH primal policies over a set of out-of sample scenarios, we consider the Wasserstein distance $\mathbf{W_2}$. This measure combines two different type of values that need to be taken into account when dealing with histograms. On one side, the distance between the probabilities of each bin and, on the other, the distances between bin values themselves.

The metric $\mathbf{W_2}$ is probably the most used distance in probability spaces, and it behaves well with discrete probabilities. In addition, when paired with a probability, the Wasserstein distance provides a metric space (see [16, Proposition 2.2]). For two distributions

$$\mu = \sum_i \mu_i \delta_{x_i}, \qquad \nu = \sum_{i=1}^{m} \nu_j \delta_{y_j},$$

the Kantorovich formulation of the Wasserstein distance is:

$$\mathbf{W_2}(\mu, \nu) = \min_{\pi \in \Pi} \sum_{i,j} \|x_i - y_j\|^2 \pi_{i,j}, \text{ where } \Pi = \Big\{ (\pi_{i,j})_{1 \leqslant i \leqslant n, 1 \leqslant j \leqslant m} : \sum_i \pi_{i,j} = \mu_j, \sum_j \pi_{i,j} = \nu_i \Big\}.$$

For this simulation we keep the fist-stage decisions: $(\nu_j^7, \nu_j^{14}, \dots, \nu_j^{7\times 52})$ that come from optimization part and simulate the cost-to-go function with new scenarios $(\mathcal{J}_j^t)$, $t \in A_w$, in the w-th week. For 200 out-of-sample scenarios, Figure 11 shows the performance of both RH and RRH in terms of distribution of the price signals.

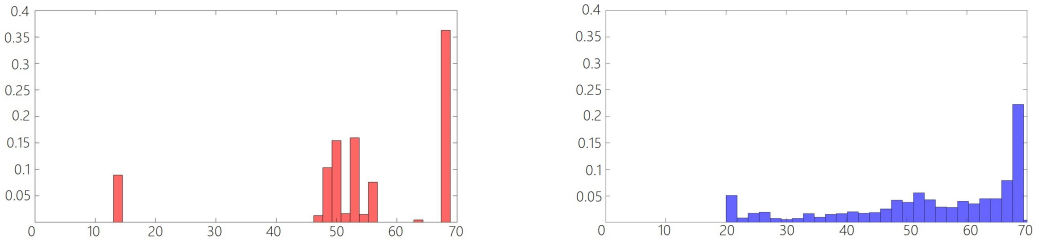

RH | RRH with $\beta = 7000$

Figure 11: Mean price signals of the first 25 weeks, simulated with primal policy of RH and RRH

In Figure 12 we see the histogram of the mean in w , for $w \in \{1, ..., 25\}$ of the price signal $\pi^{\beta,s,w}$ ($\beta = 0$ for RH, and $\beta = 7000$ for RRH). The histogram represents the distribution with respect to scenarios s.

We observe that the regularized price signal has a smooth distribution, and RRH is less susceptible than RH to variations of different samples. The right graph in Figure 11 is repeated on the left in Figure 12, to contrast the difference in RRH's price distribution when increasing the regularization parameter (on the right, $\beta = 100000$).

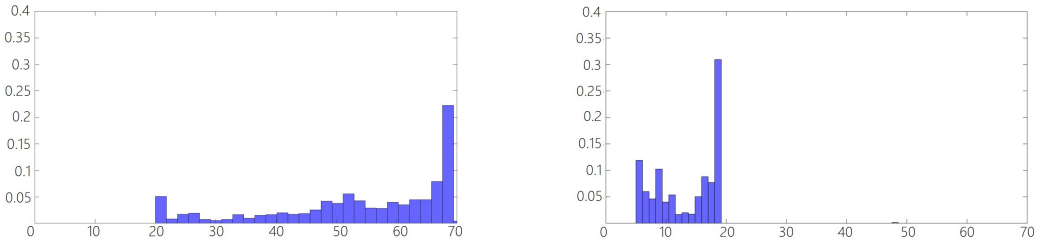

RRH with $\beta = 7000$ RRH with $\beta = 100000$

Figure 12: Mean price signals, simulated with RRH primal policy with two different values for β

In Figure 12 we see a comparison between the histogram of the mean in w , for $w \in \{1, ..., 25\}$ of the price signal $\pi^{\beta,s,w}$ ($\beta = 7000$, and $\beta = 10000$ for RRH).

In the right histogram in Figure 12 the shift to the left indicates a reduction in the price signals. This is in agreement with the optimization phase: with the primal policy, the higher β, the lower the reservoir levels. Table 4 shows the expected value and variance of the rolling-horizon variants.

	RH	RRH ($\beta = 7000$)	RRH ($\beta = 100000$)
Mean Value	61.22	54.93	13.8
Standard Deviation	16.2	14.31	11.34

Table 4: Price signal mean and deviation for one primal simulation with inflow scenarios following the log-normal distribution.

In order to evaluate the variability of the approaches under 15 different samples, in Table 5 we measure the variation of the distributions using the Wasserstein distance. The figures in Table 5 show a clear drop in the standard deviation for RRH, reflected also in the Wasserstein distance.

	RH	RRH ($\beta = 7000$)
Mean (Samples)	61.28	53.95
Standard Deviation (Samples)	16.38	14.40
Wasserstein Distance	28.16	15.78

Table 5: Price signal mean and deviation over different primal policies, first 25 weeks with inflow scenarios following the log-normal distribution.

Our final Figure 13, with the level of the reservoirs in the balancing zone NO2 (Norway) shows a typical behavior, observed for all the hydro-plants, with RH exhibiting a more erratic management of the water and keeping lower levels, when compared to RRH. The reason why we see apparently just one blue line is that all paths have close first-stage decisions.

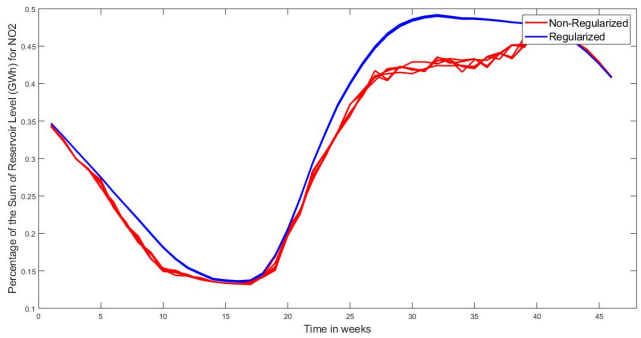

Figure 13: Water management of NO2 with primal simulation

5.2.2 Dual Simulation

The dual policies (33) provided by RH and RRH, are compared with the cuts for the future-cost functions obtained at the optimization phase with SDDP. Using the same set of scenarios employed in the primal simulation reported in Figure 11, we obtain the output in Figure 14. We note that prices vary between 0 and 100 for all approaches, with both SDDP and RH concentrating prices mostly in extreme values and RRH having a better price distribution.

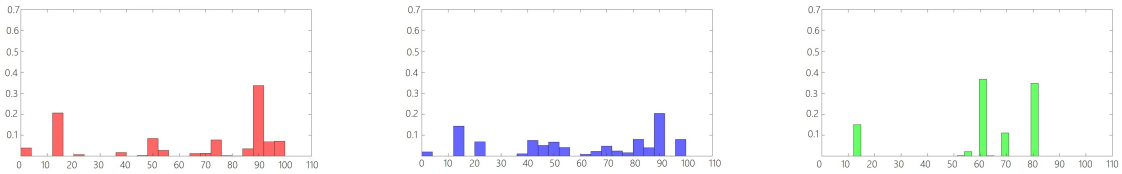

RH RRH SDDP

Figure 14: Mean price signals of the first 25 weeks with dual simulation

The variability of the approaches under different samples, is reported in Table 6. Like with the primal policy in Table 5, we observe once again, though this time with less expressive results, more stability for RRH. Contrary to SDDP, the regularization approach RRH was able to reduce the distance between histograms while keeping the expected value close to the one with RH.

	SDDP	RH	RRH ($\beta = 7000$)
Mean (Samples)	68.2	57.93	58.08
Standard Deviation (Samples)	34.5	38.48	30.1
Wasserstein Distance (Mean of pairwise distances)	6.11	5.64	4.46

Table 6: Price signal mean and deviation over different dual policies, first 25 weeks

We finish our analysis comparing in Figure 15 different paths of the first-stage primal decision that is, the level of reservoirs. Each path consists of a different sequence of scenarios. Each line represents a path and each color a different algorithm.

The behavior of the approaches is similar to that obtained with the primal simulation. Again, different SDDP paths exhibit stronger variation than those computed by RH and RRH. This is coherent with the fact that SDDP prices vary the most. When confronted to a sequence of more favorable scenarios, SDDP is forced to a change, with respect to its initial conservative perspective.

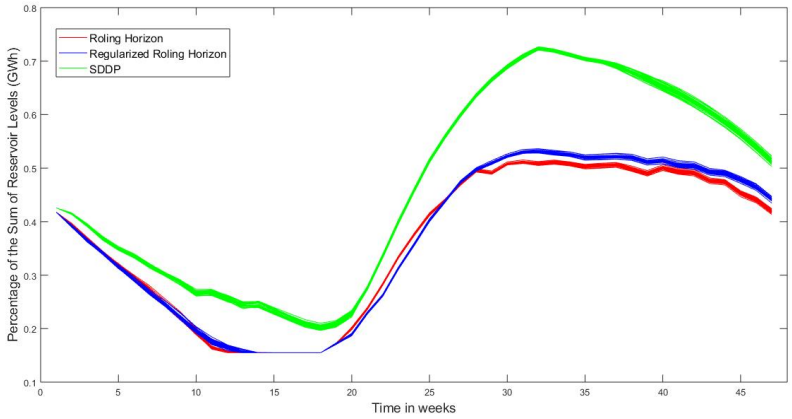

Figure 15: Reservoir dynamics

In Figure 15 we observe that, for RH and RRH, the reservoir levels In terms of quality of the output under simulation, our RRH approach seems to be more stable for the considered sets of runs.

To conclude, we note that the best choice for the penalization/regularization parameter is clearly problem dependent. In our runs, setting its value to $\beta = 7000$ was driven by the constraint violation percentage, inferior to 1%, for the water balance equation.

Concluding Remarks

In many applications dual variables are an important output of the solution process, due to their role as price signals. In stochastic programming problems, price signals are distributions depending on the input scenarios, such as rain estimations. This uncertainty makes future prices vulnerable with respect to the robustness and quality of the sample of scenarios. With the approach proposed in this work, the computed prices do not exhibit much sensitivity to samples.

In energy generation, the price signal distribution is used in long-term planning, and the mean is usually a price indicator of forward contracts. Our computational experience, both proof-of-concept and on a real-life problem of ENGIE, shows the benefits of the dual regularization methodology regarding sample-insensitivity. The price to pay for that gain is to accept some level of violation of the constraints that are dualized. This is clearly a problem dependent issue, and to achieve a good compromise, the value of the parameter β should strike a balance between the improvement obtained in the SIP and the constraint violation.

Acknowledgement

The authors thank the Editor and the referees for beneficial comments that helped to improve the paper.

Data availability statement

The dataset analysed during the current study is not publicly available, being property of ENGIE.

The authors declare that they do not have conflict of interest of any kind.

References

[1] A. Bischi, L. Taccari, E. Martelli, E. Amaldi, G. Manzolini, P. Silva, S. Campanari, and E. Macchi. "A rolling-horizon optimization algorithm for the long term operational scheduling of cogeneration systems". In: *Energy* 184 (2019), pp. 73–90.

[2] A. L. Dontchev and R. T. Rockafellar. *Implicit functions and solution mappings: A view from variational analysis*. Springer, 2014.

[3] L. F. Escudero, J. L. de la Fuente, C. Garcia, and F. J. Prieto. "Hydropower generation management under uncertainty via scenario analysis and parallel computation". In: *IEEE Transactions on Power Systems* 11.2 (1996), pp. 683–689.

[4] A. Gjelsvik, B. Mo, and A. Haugstad. "Long- and Medium-term Operations Planning and Stochastic Modelling in Hydro-dominated Power Systems Based on Stochastic Dual Dynamic Programming". In: *Handbook of Power Systems I*. Ed. by P. Pardalos, S. Rebennack, M. Pereira, and N. Iliadis. Springer, 2010, pp. 33–55.

[5] I. Goodfellow, Y. Bengio, and A. Courville. *Deep Learning*. MIT Press, 2016.

[6] G. Hechme-Doukopoulos, S. Brignol-Charousset, J. Malick, and C. Lemaréchal. "The short-term electricity production management problem at EDF". In: *Optima Newsletter - Mathematical Optimization Society* 84 (Oct. 2010), pp. 2–6.

[7] J. L. Higle and S. Sen. "Finite master programs in regularized stochastic decomposition". In: *Mathematical Programming* 67.1 (1994), pp. 143–168.

[8] K. Hoyland and S. Wallace. "Generating scenario trees for multistage decision problems". In: *Management Science* 47 (2001), pp. 295–307.

[9] A. J. King and R. T. Rockafellar. "Sensitivity analysis for nonsmooth generalized equations". In: *Mathematical Programming* 55.1 (1992), pp. 193–212.

[10] B. Kummer. "Generalized equations: Solvability and regularity". In: *Sensitivity, Stability and Parametric Analysis*. Vol. 21. Mathematical Programming Studies. Springer Berlin Heidelberg, 1984, pp. 199–212.

[11] C. Lage, C. Sagastizábal, and M. Solodov. "Multiplier Stabilization Applied to Two-Stage Stochastic Programs". In: *Journal of Optimization Theory and Applications* 183.1 (2019), pp. 158–178.

[12] Y. Liu, H. Xu, and G.-H. Lin. "Stability Analysis of Two-Stage Stochastic Mathematical Programs with Complementarity Constraints via NLP Regularization". In: *SIAM Journal on Optimization* 21 (2011), pp. 669–705.

[13] V. L. de Matos and E. C. Finardi. "A computational study of a stochastic optimization model for long term hydrothermal scheduling". In: *International Journal of Electrical Power & Energy Systems* 43.1 (2012), pp. 1443–1452.

[14] A. Philpott and V. de Matos. "Dynamic sampling algorithms for multi-stage stochastic programs with risk aversion". In: *European Journal of Operational Research* 218.2 (2012), pp. 470–483.

[15] M. V. F. Pereira and L. M. V. G. Pinto. "Multi-stage stochastic optimization applied to energy planning". In: *Mathematical Programming* 52.1 (1991), pp. 359–375.

[16] G. Peyré and M. Cuturi. "Computational optimal transport: with applications to data science". In: *Foundations and Trends in Machine Learning* 11.5-6 (2019), pp. 355–607.

[17] R. Rockafellar and R. J.-B. Wets. *Variational Analysis*. Heidelberg, Berlin, New York: Springer Verlag, 1998.

[18] A. Shapiro, D. Dentcheva, and A. Ruszczyński. *Lectures on Stochastic Programming: Modeling and Theory*. Ed. by M. P. Society. MPS–SIAM Series on Optimization. SIAM - Society for Industrial and Applied Mathematics, 2009, p. 436.

[19] R. van Slyke and R.-B. Wets. "L-shaped linear programs with applications to optimal control and stochastic programming". In: *SIAM Journal of Applied Mathematics* 17 (1969), pp. 638–663.

[20] A. Street, A. Brigatto, and D. M. Valladão. "Co-Optimization of Energy and Ancillary Services for Hydrothermal Operation Planning Under a General Security Criterion". In: *IEEE Transactions on Power Systems* 32.6 (2017), pp. 4914–4923.

[21] S. W. Wallace and S.-E. Fleten. "Stochastic Programming Models in Energy". In: *Stochastic Programming*. Vol. 10. Handbooks in Operations Research and Management Science. Elsevier, 2003, pp. 637–677.

[22] S. Zaourar and J. Malick. "Prices stabilization for inexact unit-commitment problems". In: *Mathematical Methods of Operations Research* 78.3 (Dec. 2013), pp. 341–359.